J Appl Electrochem (2012) 42:875–881
DOI 10.1007/s10800-012-0461-x

ORIGINAL PAPER

Engineering graphene/carbon nanotube hybrid for direct electron transfer of glucose oxidase and glucose biosensor

Jianli Chen · Xianliang Zheng · Fujun Miao · Jienan Zhang · Xiaoqiang Cui · Weitao Zheng

Received: 18 May 2012 / Accepted: 22 July 2012 / Published online: 5 August 2012

Abstract The graphene/carbon nanotube hybrid was designed and implemented by a deoxygenation process for direct electron transfer of glucose oxidase and glucose biosensor. The procedure was analyzed by transmission electron microscopy, X-ray photoelectron spectroscopy, and Raman spectra, etc. The strategy of structurally engineering one-dimensional carbon nanotube (CNT) and two-dimensional graphene oxide (GO) presented three benefits: (a) a deoxygenation process between GO and acid-CNT was introduced under strongly alkaline condition; (b) GO prevented the irreversible integration of CNT; and (c) CNT hindered the restacking of GO. The RGO interacted with CNT through the van der Waals forces and π–π stacking interaction. The three-dimensional hybrid not only had a high surface area, but also exhibited a good electronic conductivity. A direct electrochemistry of glucose oxidase was obtained on the nanohybrid modified electrode which showed good response for glucose sensing. This study would provide a facile and green method for the preparation of nanohybrid for a wide range of applications including biosensing, super capacitor, and transparent electrode.

Keywords Graphene · Carbon nanotube · Glucose oxidase · Three-dimensional hybrid · Biosensor · Direct electrochemistry

J. Chen · X. Zheng · F. Miao · J. Zhang · X. Cui (✉) · W. Zheng (✉)
Department of Materials Science, Key Laboratory of Automobile Materials of MOE and State Key Laboratory of Superhard Materials, Jilin University, Changchun 130012, People's Republic of China
e-mail: xqcui@jlu.edu.cn

W. Zheng
e-mail: wtzheng@jlu.edu.cn

1 Introduction

Direct electron transfer (DET) is an important way of achieving protein electron transfer between active centers and the supporting substrate in biological systems, electrochemical biosensors, and bioelectronics devices [1–4]. However, having the active sites deeply buried within electrically well-insulated prosthetic shells, it is difficult to achieve protein DET from the active sites to the electrode surface [5]. Considerable attention has been attracted to develop new and high-performance enzymatic electrochemical biosensors. But there still remains a challenge to explore appropriate supporting matrixes for promoting DET behaviors. Nanomaterials, including carbon nanomaterials [6–8], noble metal nanoparticles [3, 9], and metal oxides [10], offer significant advantages for enhancing protein DET capacity and fabrication of high-performance biosensors due to their small size, high surface area, as well as high conductivity.

Recently, owing to their unique electrical and mechanical properties as well as large surface area, carbon-based materials ranging from zero-dimensional (0D) fullerene, one-dimensional (1D) carbon nanotube, to two-dimensional (2D) graphene have attracted more attention for potential applications in biosensors [11–15], solar cells, supercapacitors [16–18], and batteries [19]. Apart from their individual properties, attempts have been made to design and engineer carbon-based hybrid materials for preparing three-dimensional (3D) architectures which have enhanced the improvement in optical and electrical properties [20, 21]. In particular, the 3D electron transfer network and high surface area have enabled the hybrid structure as a promising platform to facilitate protein DET. A number of methods to synthesize CNT/graphene have been reported, including chemical vapor deposition [22, 23] and layer-by-layer

assembly [17, 21, 24]. The hybrid structure prepared by CVD is highly hydrophobic that prevents the protein absorption and is unsuitable for further modification and functionalization. High electrical conductivity is also a key factor for the high performance of electrochemical biosensors. It is necessary to increase the conductivity of hybrid structure when utilizing chemical approach to assemble hybrid structure.

In this study, we report a facile and green strategy to prepare a 3D carbon nanotube (CNT)/graphene hybrid. The mixture of acid-CNT and graphene oxide (GO) by sonication shows a homogeneous distribution with good stability based on the van der Waals forces or π–π stacking interaction [25, 26]. In the mean time, a deoxygenation process between GO and acid-CNT is introduced under strongly alkaline condition. GO can hinder the irreversible aggregation of CNT; meanwhile, CNT can hinder the restacking of GO. This 3D hybrid not only has a high surface area, but also exhibits a good electronic conductivity. The as-prepared nanohybrid displays an interconnected network of MWNTs with well-defined nanopores, which is beneficial to the electron transport and direct electrochemistry of glucose oxidase as an electrode for glucose sensing.

2 Materials and methods

2.1 Materials

Graphite powder, 325 meshes, 99.9995 % (metals basis), was obtained from Alfa Aesar. $NaNO_3$ (99.0 %), H_2SO_4 (98 wt%), H_2O_2 (30 wt%), HCl (37 wt%), and $KMnO_4$ (99.5 %) were obtained from Tianjin Guangfu Chemical Reagent Co., Ltd. Glucose oxidase (GOD) was purchased from Sinopharm Chemical Reagent Co., Ltd. (Shanghai, China). The CNTs (with 95 % purity) were obtained from Shenzhen Nanotech Port Co., Ltd. (Shenzhen, China). All reagents were used as received without further purification. MilliQ water (18.2 Ω cm^{-1}) was used to make aqueous solutions. All glasswares used in the following procedures were cleaned in freshly prepared HNO_3/HCl (1:3) solution, thoroughly rinsed with water, and dried in air.

2.2 Instrumentation

The morphology of the products was characterized by scanning electron microscopy (SEM, JEOL JSM-6700F operated at 8 kV) and transmission electron microscope (TEM, JEOL JEM-2100F operated at 200 kV). The Raman spectrum was detected with a Renishaw 1000 microspectrometer connected to a Leica microscope with an objective lens of 50× (NA = 0.5). The spectra were obtained under a laser power of 5 mW, an accumulation time of 30 s, and an excitation wavelength of 514.5 nm.

The cyclic voltammetry (CV) and electrochemical impedance measurements were carried out on a CHI650D electrochemical workstation (Shanghai, Chenhua Co., China), with a three-electrode cell. A glassy carbon electrode (3 mm in diameter) was used as the working electrode. A Pt wire served as the counter electrode, and a saturated calomel electrode (SCE) was used as the reference electrode.

2.3 Synthesis of reduced graphene oxide/carbon nanotube hybrid materials (RGO-CNT)

GO was synthesized directly from graphite according to the modified Hummers method. The resulting solid was dried in air and diluted to make graphene oxide dispersion (0.25 mg ml^{-1}) with the aid of sonication. And CNTs were refluxed in a mixture of concentrated nitric acid and sulfuric acid (1:3, v/v) at 60 °C for 3 h, filtered, and washed with double-distilled water before using. The obtained solid was redispersed in water with a concentration of 0.25 mg ml^{-1}. The deoxygenation process was carried out under strongly alkaline condition [27]. For example, the mixture of GO suspension (4 ml) and acid-carbon nanotubes suspension (l ml) was ultrasonicated at 60 °C for 2 h with 4 µl KOH solution (4 M). Samples were then separated by intensive centrifugation (16,000 rpm, 2 h), followed by filtrating and washing with distilled water. For comparison, reduced GO was prepared according to the process described above without the addition of CNT. The obtained solid was redispersed in deionized water with a concentration of 1.0 mg ml^{-1}.

2.4 Preparation of RGO–CNT modified electrode and GOD-RGO–CNT electrode

The GCE was polished using 0.3 and 0.05 µm alumina powders, rinsed thoroughly with deionized water between each polishing step, sequentially sonicated in ethanol, and deionized water, and dried at room temperature. Six microliters of the suspension was dropped on the surface of GCE and dried in air. GOD was assembled on RGO–CNT by dipping the RGO–CNT/GC electrode in the enzyme solution (2.0 mg ml^{-1} in PBS) at 4 °C for overnight. Afterward, the GOD-RGO–CNT/GC electrode was thoroughly rinsed with PBS solution and double-distilled water, and stored in 4 °C. The GOD-RGO/GC and GOD-CNT/GC electrodes were fabricated using similar procedure as GOD-RGO-CNT/GC electrode.

3 Results and discussion

As shown in Fig. 1a, FTIR spectra of CNT and acid-CNT reveal the C=O and C–O stretching vibration bands at 1,730 and 1,039 cm^{-1}, indicating that oxygen functional

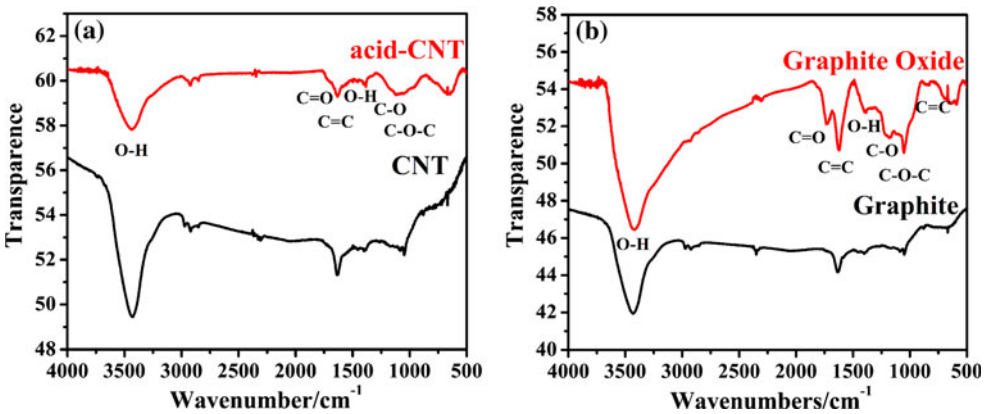

Fig. 1 FTIR spectra of the **a** CNT and acid-CNT **b** graphite and graphite oxide

groups are introduced into the surface of CNT. Figure 1b displays the FTIR spectra of graphite and graphite oxide prepared by a modified Hummer's method. The characteristic peaks of graphite oxide appear at ~3420 and 1393 cm^{-1} (O–H stretching vibrations), 1726 cm^{-1} (C=O stretching), 1621 cm^{-1} (unoxidized sp^2 C–C bonds), 1220 cm^{-1} (C–OH stretching vibrations), and 1050 cm^{-1} (stretching vibrations of C–O–C). The FTIR spectra confirm the existence of oxygenous groups on acid-CNT and graphite oxide. Therefore, the deoxygenation progress will happen between acid-CNT and GO during the mixing and ultrasonicating treatment, and GO will be changed to reduced GO (RGO) at the same time. The RGO–CNT hybrid is formed because of the van der Waals forces, π–π stacking interaction, and the deoxygenation reaction [26].

The morphology of RGO–CNT is analyzed by SEM and TEM. As shown in Fig. 2, CNTs are uniformly distributed on the smooth surface of GO, while the graphene still retains few layers character thanks to the adsorption of CNTs, which prevents the stacking and scrolling effects when GO is reduced. RGO and CNT are prone to stacking together and form a 3D hybrid after the process of ultrasonic mixing and deoxygenation.

In order to indicate the reduction of the mixture of GO and acid-CNT, the XPS spectra of the mixture before and after the deoxygenation are detected as shown in Fig. 3. For the C1s spectrum of the mixture before deoxygenation (Fig. 3a), the band at 284.6 eV is in agreement with the sp^2-bonded carbon. Peaks at 286.4, 287, and 288.7 eV are assigned to the C1s of C–OH, C=O, and O=C–OH, respectively [28]. After ultrasonication under alkaline condition, the C1s spectrum of the mixture in Fig. 3b clearly indicated that most of the oxygenated functional groups are successfully removed.

Raman spectroscopy is a powerful technique to characterize the structure of carbon-based materials. Typical Raman spectra of acid-CNT, GO, RGO, and RGO–CNT obtained at an excitation wavelength of 514 nm are shown in Fig. 4. All carbon materials exhibit a D-band around 1,350 cm^{-1} assigned to the breathing mode of κ-point phonons, a G-band around 1,580 cm^{-1} attributed to the tangential stretching mode of the E2g phonon of sp^2 atoms, and a 2D-band around

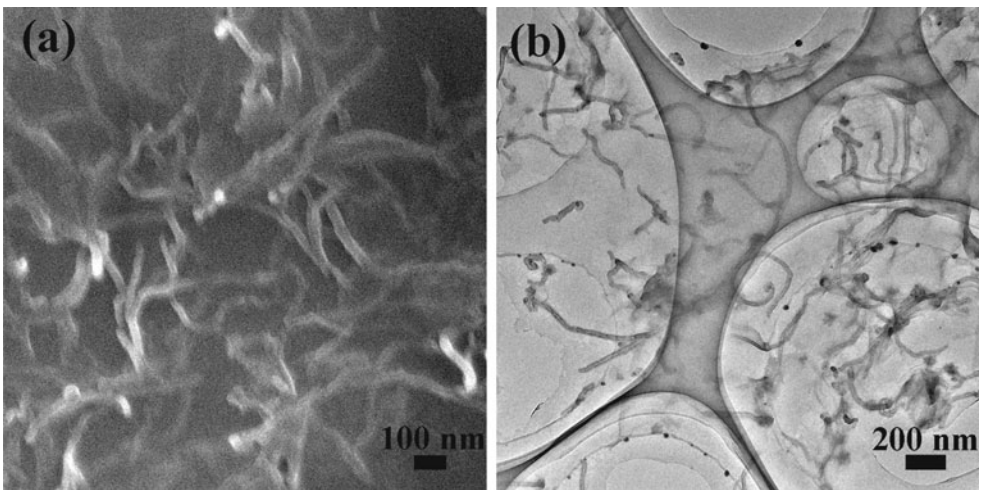

Fig. 2 SEM (**a**) and TEM (**b**) images of RGO–CNT nanohybrid

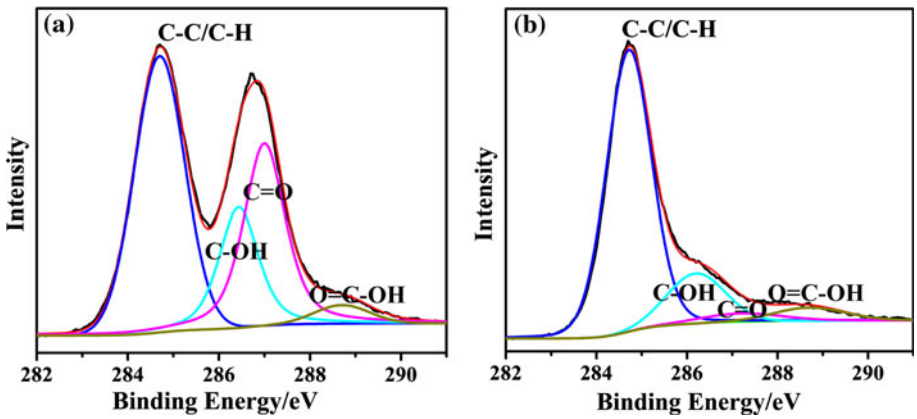

Fig. 3 The C1s XPS spectra of the mixture of GO and acid-CNT **a** before and **b** after the deoxygenation

2,700 cm^{-1} arising from a double resonance process [28, 29]. 2D-band at 2,700 cm^{-1} with no shoulder at 2,680 cm^{-1} confirmed that graphene employed in this work has only a few layers [30]. The I_D/I_G ratio is an indication of disorder and graphitization [28]. The I_D/I_G ratios of acid-CNT, GO, RGO, and RGO–CNT are 1.06, 0.85, 0.94, and 0.96, respectively. A small increase of the ratio in RGO demonstrates a decrease in the average size of the sp^2 domains upon reduction of the exfoliated GO compared to that in GO [31, 32]. RGO–CNT shows a D/G intensity ratio between RGO and acid-CNT, which suggests the formation of RGO–CNT complex.

In order to ensure restoration of the conductivity upon reduction, the carbon-based materials have been determined by electrochemical impedance spectroscopy (EIS) [2]. The corresponding Nyquist plots of EIS for GO/GC, RGO/GC, CNT/GC, and RGO-CNT/GC are shown in Fig. 5. The semicircle corresponds to the electron transfer limited process. The electron transfer resistance (Rct) at the electrode surface is calculated from the diameter of the semicircle diameter using a Randles circuit [2]. The Rct of the RGO (585 Ω) was much smaller than that of GO (1,586 Ω), which indicated that oxygenous groups have been removed. The result confirmed that the deoxygenation of GO under alkaline condition is an effective reduction method to restore the conductivity of GO. The acid-CNT has good conductivity. Thus after mixing, the Rct of RGO–CNT decreased to 386 Ω. These results, combined with the XPS, SEM, XRD, XPS, and Raman, confirm the formation of nanohybrid with 3D electron transfer structure.

As we know, GO can undergo a fast deoxygenation in strong alkaline solutions as reported in the literature [27]. Upon this purpose, we introduced functional groups to the CNT by an acid treatment. The process of the deoxygenation is also supposed to happen in a mixture of acid-CNT and GO with abundance of functional groups in the same condition [27]. The synthesis procedure is summarized in Scheme 1. In a mixture of GO and acid-CNT, GO and acid-CNT bonded together because of the van der Waals forces and π–π stacking interaction. The process of deoxygenation reaction also occurred among the oxide groups of the GO and acid-CNT. As a result of the removal of the oxide groups and the interaction for the GO and acid-CNT,

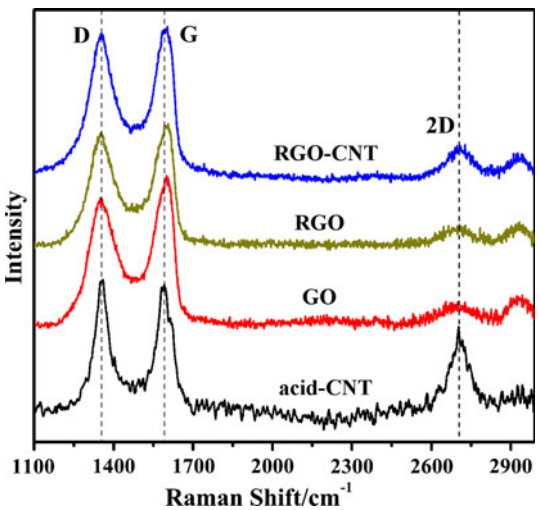

Fig. 4 Raman spectra of acid-CNT, GO, RGO, and RGO-CNT

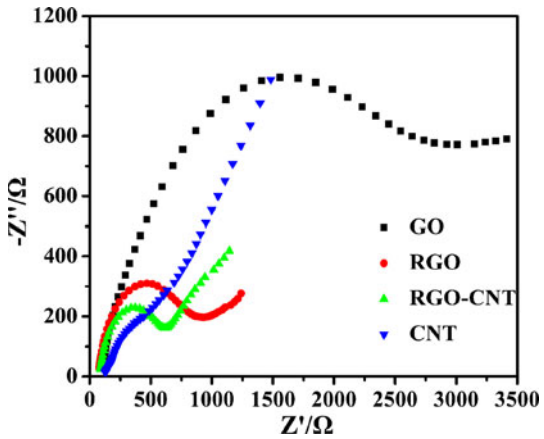

Fig. 5 Nyquist plots of EIS for GO, RGO, CNT, and RGO-CNT. EIS was performed in a 0.1 M KCl solution containing 2 mM $K_3[Fe(CN)_6]$ + 2 mM $K_4[Fe(CN)_6]$ (1:1). Frequency: 0.1 Hz–10 kHz

the hybrid structure with 3D electron transfer network and high surface area has been built for DET.

The direction electrochemistry of GOD is obtained on the as-prepared RGO–CNT nanohybrids as shown in Fig. 6, which presents CVs of RGO–CNT/GC (a), RGO–CNT-GOD/GC (b), and CNT-GOD/GC (c) in 0.1 M PBS solution saturated with N_2 at a scan rate of 0.05 V s^{-1}. A pair of redox peaks at −0.488 and −0.513 V was observed at RGO–CNT-GOD/GC, indicating DET between the cofactor FAD of GOD and the modified electrode. The peak potential separation is about 25 mV at a scan rate of 0.05 V s^{-1}. The formal potential is −0.501 V, which is close to the standard electrode potential for GOD [33]. This indicates that the GOD immobilized on the modified electrode still retains its bioactivity. The increased background current should be caused by the high-capacitance current of partially reduced RGO–CNT. The direct electrochemistry was obtained on a CNT-GOD/GCE. It is maybe due to the fact that CNTs are tending to form bundle structure that blocks the GOD immobilization and the electron transfer. The presence of GO can hinder the irreversible aggregation of CNT; meanwhile, CNTs can hinder the restacking of GO. This 3D hybrid provides high surface area and good electronic conductivity, which is suitable for GOD to achieve DET.

CVs of RGO–CNT-GOD/GCE at various scan rates were also investigated as shown in Fig. 7. The relationship of redox peak current with the scan rate was calibrated with linear regression equation as $I_{pa} = 0.03855 + 0.00598v$, $r = 0.9989$, and $I_{pc} = -0.08541–0.00768v$, $r = 0.9991$. The peak currents linearly increased with the increasing scan rate, indicating a surface-controlled process. These results demonstrated that the special nanostructure can promote the DET reaction of GOD.

Figure 8 shows the CVs of RGO–CNT-GOD/GCE in 0.1 M PBS solution with various concentrations of

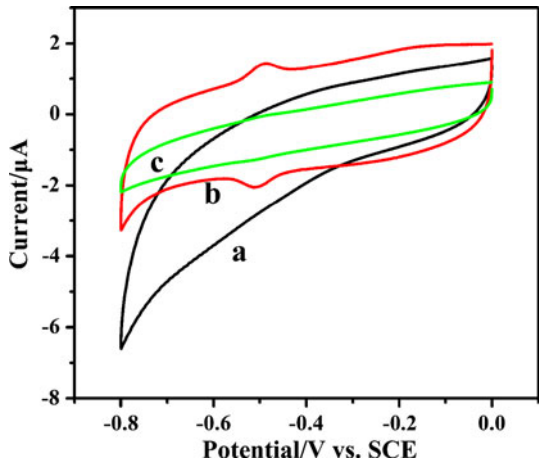

Fig. 6 CVs of RGO–CNT/GC (**a**), RGO–CNT-GOD/GC (**b**), and CNT-GOD/GC (**c**) in 0.1 M PBS solution saturated with N_2 at a scan rate of 0.05 V s^{-1}

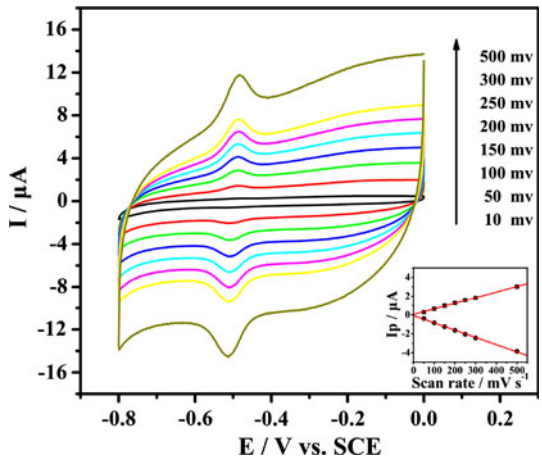

Fig. 7 CVs of RGO–CNT-GOD/GC at various scan rates from 0.01, 0.05, 0.1, 0.15, 0.2, 0.25, and 0.3–0.5 V s^{-1}, respectively. *Inset* The plots of peak current versus scan rate

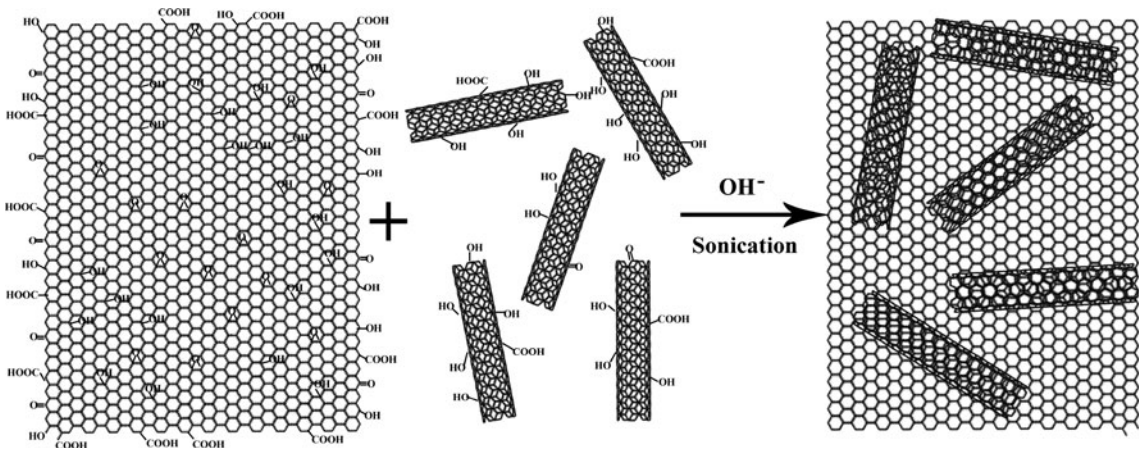

Scheme 1 Procedure of RGO–CNT nanohybrid preparation

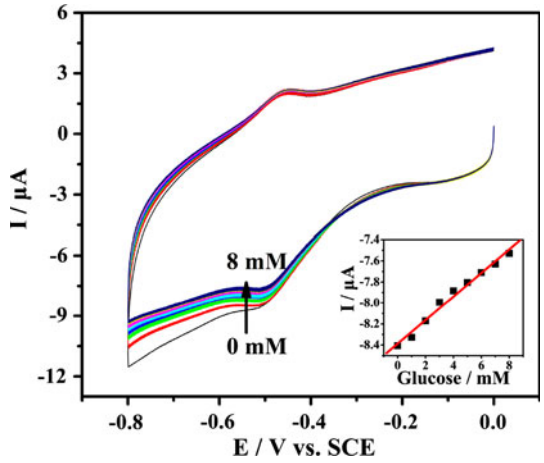

Fig. 8 CVs of RGO–CNT-GOD/GC in 0.1 M PBS solution with various concentrations of glucose saturated with air 0.1 V/s. The inset is the calibration curve corresponding to amperometric responses at −0.5 V

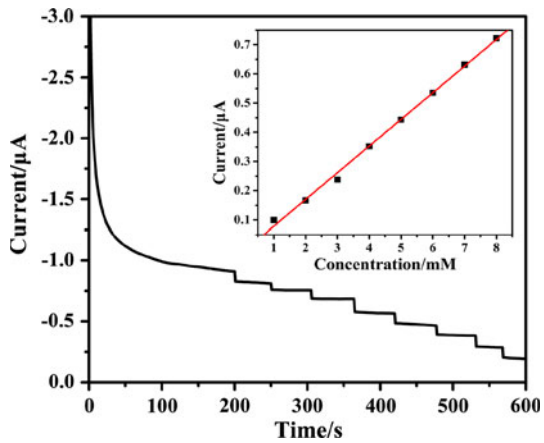

Fig. 9 Amperometric *i–t* response of RGO–CNT-GOD/GC in 0.1 M PBS solution with various concentrations of glucose saturated with air. Applied potential: −0.45 V. The *inset* is the calibration curve for glucose detection

air-saturated glucose. The inset is a calibration curve corresponding to amperometric responses at −0.5 V. The current achieves the highest value in air-saturated PBS without glucose. The response displays a linear relationship up to 8 mM. This can be attributed to the electrocatalytic response to dissolved oxygen [10]. In order to investigate the performance of the RGO–CNT modified electrode for the glucose electrochemical oxidation, amperometric *i–t* response with addition of various concentrations of glucose was studied in 0.1 M PBS solution saturated with air at −0.45 V (Fig. 9). The current decreases for each addition of glucose. The 3D glucose biosensor shows a sensitivity of 1.27 μA mM^{-1} cm^{-2} and a fast response time of less than 4 s, which is close to the glucose biosensor by a simple electrochemical approach for the immobilization of glucose oxidase on reduced graphene oxide [34]. The response current remains 90 % of the original value after one week when the modified electrode was stored at 4 °C.

4 Conclusions

We report a facile and green strategy to prepare a 3D CNT/graphene hybrid based on the van der Waals forces or π–π stacking by introducing a deoxygenation process between GO and acid-CNT under strongly alkaline condition. The 3D RGO–CNT structure was designed by engineering 1D CNT and 2D GO, in which GO will prevent the irreversible integration of CNT and CNT will hinder the restacking of GO. This hybrid not only has a high surface area, but also exhibits a good electronic conductivity. This strategy for the preparation of 3D electron materials is simple and low-cost, and the deoxygenation reaction between GO and acid-CNT under alkaline condition provide a new green route. A direct electrochemistry of GOD is obtained on the nano-hybrid modified electrode, which shows good response for glucose sensing.

Acknowledgments This work was financially supported by the National Natural Science Foundation of China (Nos. 21075051, 21143008 and 50832001), Program for New Century Excellent Talents in University (NCET-10-0433), the "211" and "985" project of Jilin University, China, and State Key Laboratory of Electroanalytical Chemistry, CIAC, CAS.

References

1. Liu Q, Lu X, Li J, Yao X, Li J (2007) Biosens Bioelectron 22:3203. doi:10.1016/j.bios.2007.02.013
2. Kang X, Wang J, Wu H, Aksay IA, Liu J, Lin Y (2009) Biosens Bioelectron 25:901. doi:10.1016/j.bios.2009.09.004
3. Wang L, Wang E (2004) Electrochem Commun 6:49. doi:10.1016/j.elecom.2003.10.004
4. Guo CX, Li CM (2010) Phys Chem Chem Phy 12:12153. doi:10.1039/c0cp00378f
5. Krajewska B (2004) Enzyme Microb Technol 35:126. doi:10.1016/j.enzmictec.2003.12.013
6. Liu Y, Wang M, Zhao F, Xu Z, Dong S (2005) Biosens Bioelectron 21:984. doi:10.1016/j.bios.2005.03.003
7. Cai C (2004) Anal Biochem 332:75. doi:10.1016/j.ab.2004.05.057
8. Wu P, Shao Q, Hu Y et al (2010) Electrochim Acta 55:8606. doi:10.1016/j.electacta.2010.07.079
9. Pingarron J, Yanezsedeno P, Gonzalezcortes A (2008) Electrochim Acta 53:5848. doi:10.1016/j.electacta.2008.03.005
10. Bao S-J, Li C-M, Zang J-F, Cui X-Q, Qiao Y, Guo J (2008) Adv Funct Mater 18:591. doi:10.1002/adfm.200700728
11. Rivas G, Rubianes M, Rodriguez M (2007) Talanta 74:291. doi:10.1016/j.talanta.2007.10.013
12. Gao Q, Guo Y, Zhang W, Qi H, Zhang C (2011) Sens Actuat B Chem 153:219. doi:10.1016/j.snb.2010.10.034
13. Akhavan O, Ghaderi E, Rahighi R (2012) ACS Nano 6:2904. doi:10.1021/nn300261t

14. Gutés A, Carraro C, Maboudian R (2012) Biosens Bioelectron 33:56. doi:10.1016/j.bios.2011.12.018
15. Pumera M, Ambrosi A, Bonanni A, Chng ELK, Poh HL (2010) Trends Anal Chem 29:954. doi:10.1016/j.trac.2010.05.011
16. Qian Y, Lu S, Gao F (2011) J Mater Sci 46:3517. doi:10.1007/s10853-011-5260-y
17. Yu D, Dai L (2010) J Phys Chem Lett 1:467. doi:10.1021/jz9003137
18. Yang SY, Chang KH, Tien HW et al (2011) J Mater Chem 21:2374. doi:10.1039/c0jm03199b
19. Yang W, Ratinac KR, Ringer SP, Thordarson P, Gooding JJ, Braet F (2010) Angew Chem Int Ed 49:2114. doi:10.1002/anie.200903463
20. Lee CH, Yang CK, Lin MF, Chang CP, Su WS (2011) Phys Chem Chem Phy 13:3925. doi:10.1039/c0cp01569e
21. Byon HR, Lee SW, Chen S, Hammond PT, Shao-Horn Y (2011) Carbon 49:457. doi:10.1016/j.carbon.2010.09.042
22. Das S, Seelaboyina R, Verma V et al (2011) J Mater Chem 21:7289. doi:10.1039/c1jm10316d
23. Yu K, Lu G, Bo Z, Mao S, Chen J (2011) J Phys Chem Lett 2:1556. doi:10.1021/jz200641c
24. Hong T-K, Lee DW, Choi HJ, Shin HS, Kim B-S (2010) ACS Nano 4:8
25. Shao G, Lu Y, Wu F, Yang C, Zeng F, Wu Q (2012) J Mater Sci 47:4400. doi:10.1007/s10853-012-6294-5
26. Zhang C, Ren L, Wang X, Liu T (2010) J Phys Chem C 114:11435
27. Fan X, Peng W, Li Y et al (2008) Adv Mater 20:4490. doi:10.1002/adma.200801306
28. Yang D, Velamakanni A, Bozoklu G et al (2009) Carbon 47:145. doi:10.1016/j.carbon.2008.09.045
29. Lee V, Whittaker L, Jaye C, Baroudi KM, Fischer DA, Banerjee S (2009) Chem Mater 21:3905. doi:10.1021/cm901554p
30. Alwarappan S, Liu C, Kumar A, Li C-Z (2010) J Phys Chem C 114:12920. doi:10.1021/jp103273z
31. Stankovich S, Dikin DA, Piner RD et al (2007) Carbon 45:1558. doi:10.1016/j.carbon.2007.02.034
32. Eda G, Chhowalla M (2010) Adv Mater 22:2392. doi:10.1002/adma.200903689
33. Wanekaya AK, Chen W, Myung NV, Mulchandani A (2006) Electroanalysis 18:533. doi:10.1002/elan.200503449
34. Unnikrishnan B, Palanisamy S, Chen SM (2012) Biosens Bioelectron. doi:10.1016/j.bios.2012.06.045